2019 American Control Conference (ACC)
Philadelphia, PA, USA, July 10-12, 2019

System Inversion for Sampled-Data Feedforward Control: Balancing On-Sample and Intersample Behavior

Jurgen van Zundert, Wataru Ohnishi, Hiroshi Fujimoto, Tom Oomen

Abstract— **Discrete-time system inversion for perfect tracking goes at the expense of intersample behavior. The aim of this paper is the development of a discrete-time inversion approach that improves continuous-time performance by also addressing the intersample behavior. The proposed approach balances the on-sample and intersample behavior and provides a whole range of new solutions, with stable inversion and multirate inversion as special cases. The approach is successfully applied to a motion system. The proposed approach improves the intersample behavior through discrete-time system inversion.**

I. Introduction

Physical systems evolve in continuous time and hence their performance is naturally defined in continuous time. Many approaches for tracking control, including inverse model feedforward and iterative learning control (ILC), are based on system inversion, see, for example [1], [2]. For continuous-time systems, system inversion approaches such as, for example, [3] can be used. However, since controllers are often implemented in a digital environment [4], discrete-time control is often used.

One of the main challenges in system inversion is non-minimum-phase behavior. Causal inversion of nonminimum-phase systems yields unbounded signals. To avoid unbounded signals, many discrete-time inversion approaches have been proposed, see, e.g., [5] for a recent overview. Approximate inversion approaches such as ZPETC, ZMETC, and NPZ-Ignore [1] are well-known, but yield limited performance due to the approximation. Optimal approaches, such as norm-optimal feedforward, $\mathcal{H}_2$-preview control, and $\mathcal{H}_\infty$-preview control [5, Sections 4.3 and 4.4], yield high performance in discrete time. Discrete-time stable inversion [5, Section 4.2] yields exact tracking at the discrete-time samples.

Discrete-time inversion approaches focus on the on-sample performance, i.e., at the discrete-time samples, occasionally resulting in poor intersample behavior, i.e., in between the samples. This holds in particular for zeros close to $z=-1$ [6], see, e.g., [7], [8]. As a consequence, the continuous-time behavior is poor. Indeed, the best on-sample performance does not always give the best continuous-time performance.

Multirate inversion [9], [10], not to be confused with multirate feedforward control [11], provides an interesting alternative to improve intersample behavior by sacrificing on-sample performance. However, the approach does not take into account the system dynamics when balancing the intersample and on-sample performance, i.e., the solution is not optimized for the system at hand. As a consequence, the continuous-time performance is generally sub-optimal.

Although many discrete-time inversion approaches exist, the balance between on-sample performance and intersample behavior is not optimized. The main contribution of this paper is a discrete-time inversion approach that finds the optimal balance between on-sample performance and intersample behavior for the purpose of continuous-time performance. The stable inversion and multirate inversion approaches are recovered as special cases. Related work includes [4], [12], [13] where synthesis-based approaches are presented. In contrast, the approach presented in this paper does not require synthesis.

The outline of this paper is as follows. In Section II, the control objective is formulated. The concept of the proposed approach is presented in Section III. Key ingredients to the approach are presented in Section IV and Section V. Based on these results, the approach is presented in Section VI. The advantages of the approach are demonstrated by application to a motion system application in Section VII. Conclusions are presented in Section VIII.

Notation. For notational convenience, single-input, single-output (SISO) systems are considered. The results can directly be generalized to square multivariable systems. Let $s^{(i)} \triangleq \frac{\mathrm{d}^i}{\mathrm{d}t^i}s$ denote the ith time-derivative of s, ρ the Heaviside operator, $\mathcal{B}(\cdot)$ a bilinear transformation, and $\mathbb{R}^b_{>a} = \{x \in \mathbb{R}^b \mid x[k] > a \text{ for all } k = 0,1,\ldots,b-1\}$. Let $\Sigma \overset{z}{=} (A,B,C,D)$ be a state-space model and define $\mathcal{T}(\Sigma,T) \overset{z}{=} (TAT^{-1}, TB, CT^{-1}, D)$.

II. Problem formulation

In this section, the control problem is formulated. The considered tracking control configuration is shown in Fig. 1, with reference trajectory $r(t) \in \mathbb{R}$, control input $u(t) \in \mathbb{R}$, output $y(t) \in \mathbb{R}$, digital controller F, sampler $\mathcal{S}$, and zero-order hold $\mathcal{H}$. The continuous-time, linear time-invariant (LTI) system H_c is given by

$$\dot{x}(t) = A_c x(t) + B_c u(t), \tag{1a}$$

$$y(t) = C_c x(t), \tag{1b}$$

with $x(t) \in \mathbb{R}^n$, $n \in \mathbb{N}$ and can be either an open-loop or closed-loop system.

Conventional discrete-time control focuses on the on-sample performance. The discrete-time system $H = \mathcal{S}H_c\mathcal{H}$

Van Zundert and Oomen are with the Eindhoven University of Technology, Dept. of Mechanical Engineering, Control Systems Technology group, The Netherlands (e-mail: j.c.d.v.zundert@tue.nl, t.a.e.oomen@tue.nl).

Ohnishi and Fujimoto are with the University of Tokyo, Kashiwanoha, Chiba, Japan (e-mail: ohnishi@ieee.org, fujimoto@k.u-tokyo.ac.jp).

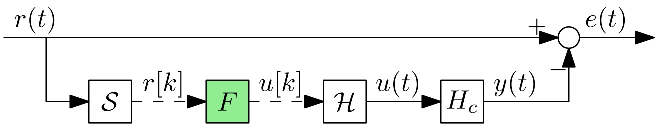

Fig. 1. Tracking control diagram with continuous-time system H_c, sampler $\mathcal{S}$, and hold $\mathcal{H}$. Given continuous-time reference trajectory $r(t)$, the objective is to minimize continuous-time error $e(t)$ through design of discrete-time controller F, while control input $u[k]$ remains bounded.

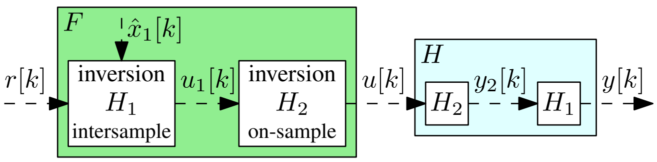

Fig. 2. The discrete-time system H is decomposed into H_1 and H_2. System H_1 is inverted such that there is exact state tracking of the desired state $\hat{x}_1[k]$ every n_1 samples for the purpose of intersample behavior. System H_2 is inverted such that there is exact output tracking every sample for the purpose of on-sample behavior.

with H_c in (1) and sampling time δ is given by

$$x[k+1] = Ax[k] + Bu[k], \tag{2a}$$

$$y[k] = Cx[k], \tag{2b}$$

with $A = e^{A_c\delta}$, $B = \int_0^\delta e^{A_c\tau} B_c \, \mathrm{d}\tau$, and $C = C_c$. In this setting, perfect on-sample tracking, i.e., $e[k] = 0$, for all k, is achieved for $F = H^{-1}$. However, this does not provide any guarantees for the intersample performance $e(t)$, $t \neq k\delta$. Hence, the continuous-time performance in terms of $e(t)$, for all t, may be poor as observed in, e.g., [7].

The control objective considered in this paper is to minimize the continuous-time error $e(t)$. Note that this includes both on-sample ($t = k\delta$) and intersample ($t \neq k\delta$) performance. Importantly, $u[k]$ should remain bounded, even in the presence of nonminimum-phase behavior. Trajectory $r(t)$ is assumed to be known a priori. In the next section, the concept of the proposed approach is presented.

III. Inversion for On-Sample and Intersample Behavior

In the proposed approach, the system is decomposed into two parts and inverted separately as illustrated in Fig. 2, where H is decomposed as $H = H_1H_2$. The inversion of system H_1 aims at the intersample behavior. More specific, let n_1 be the state dimension of H_1, then H_1 is inverted such that there is exact state tracking of a desired state $\hat{x}_1[k]$ every n_1 samples. The inversion of H_2 aims at the on-sample behavior through perfect output tracking for every sample.

Exact state tracking is experienced to yield good intersample behavior in multirate inversion [9], whereas exact output tracking yields good on-sample behavior in stable inversion [5]. Hence, the choice of the decomposition into H_1 and H_2 can be used to balance the on-sample behavior and the intersample behavior to the benefit of the continuous-time performance. The idea is conceptually illustrated in Fig. 3. An important observation is that a small on-sample error does not necessarily yield a small continuous-time error. The figure shows that the proposed approach provides a whole range of solutions that were non-existing before. The stable inversion and multirate inversion solution are recovered as the two extreme cases, see also Section VI-B.

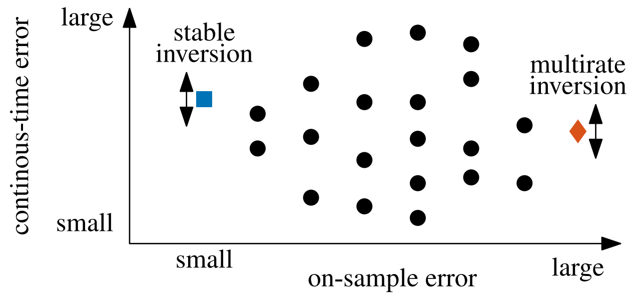

Fig. 3. Qualitative plot of the continuous-time versus on-sample error. The proposed approach balances the intersample and the on-sample behavior for the purpose of continuous-time performance. It provides a whole range of solutions that were non-existing before. Importantly, the smallest on-sample error does not necessarily yield the smallest continuous-time error as the intersample behavior may be poor. The relative performance depends on the particular settings, e.g., the system dynamics, and may vary. Stable inversion (■) and multirate inversion (♦) are recovered as special cases.

The proposed approach requires the decomposition $H = H_1H_2$ in terms of state-space realizations and the desired state $\hat{x}_1[k]$ for H_1, see also Fig. 2. In Section IV, the desired state for the continuous-time system H_c is presented. In Section V, the state-space decomposition $H = H_1H_2$ is presented. Based on these results, the complete approach is presented in Section VI.

IV. Desired State for Continuous-Time System

In this section, the desired state for the continuous-time system is presented. Given a continuous-time reference trajectory $r(t)$ together with its $n-1$ time derivatives and system H_c in (1), the objective is to determine a bounded state $\hat{x}(t)$ such that $y(t) = C_c\hat{x}(t)$ yields $y^{(i)}(t) = r^{(i)}(t)$, $i = 0, 1, \ldots, n-1$, where $(\cdot)^{(i)}$ denotes the ith time derivative of $(\cdot)$, i.e., such that $\bar{r}(t) = \bar{y}(t)$ where

$$\bar{r}(t) = \begin{bmatrix} r^{(0)}(t) \\ r^{(1)}(t) \\ \vdots \\ r^{(n-1)}(t) \end{bmatrix}, \qquad \bar{y}(t) = \begin{bmatrix} y^{(0)}(t) \\ y^{(1)}(t) \\ \vdots \\ y^{(n-1)}(t) \end{bmatrix}. \tag{3}$$

A similar approach as in [9] is used based on the controllable canonical form given by Lemma 1, see also [14, Section 17.6]. The desired state is given by Theorem 2.

Lemma 1 (Controllable canonical form)**.** *Let the transfer function of H_c in* (1) *be given by*

$$H_c(s) = C_c(sI - A_c)^{-1}B_c = \frac{B(s)}{A(s)}, \tag{4a}$$

$$A(s) = \frac{s^n + a_{n-1}s^{n-1} + \ldots + a_0}{b_0}, \tag{4b}$$

$$B(s) = \frac{b_m s^m + b_{m-1}s^{m-1} + \ldots + b_0}{b_0}, \tag{4c}$$

$b_0 \neq 0$, *then the controllable canonical form* $H_{ccf}(s) = \mathcal{T}(H_c, T_{ccf})$ *is given by*

$$\dot{x}_{ccf}(t) = A_{ccf}x_{ccf}(t) + B_{ccf}u(t), \quad (5a)$$

$$y(t) = C_{ccf}x_{ccf}(t), \quad (5b)$$

where

$$\left[\begin{array}{c|c} A_{ccf} & B_{ccf} \\ \hline C_{ccf} & \end{array}\right] = \left[\begin{array}{ccccc|c} 0 & 1 & 0 & \cdots & 0 & 0 \\ 0 & 0 & 1 & \cdots & 0 & 0 \\ \vdots & \vdots & \vdots & \ddots & \vdots & \vdots \\ 0 & 0 & 0 & \cdots & 1 & 0 \\ -a_0 & -a_1 & -a_2 & \cdots & -a_{n-1} & b_0 \\ \hline 1 & \frac{b_1}{b_0} & \frac{b_2}{b_0} & \cdots & 0 & \end{array}\right] \quad (5c)$$

$$T_{ccf}^{-1} = \begin{bmatrix} B_c & A_cB_c & \cdots & A_c^{n-1}B_c \end{bmatrix} \begin{bmatrix} \frac{a_1}{b_0} & \frac{a_2}{b_0} & \cdots & \frac{1}{b_0} \\ \frac{a_2}{b_0} & \frac{a_3}{b_0} & \cdot^{\cdot^{\cdot}} & 0 \\ \vdots & \cdot^{\cdot^{\cdot}} & \cdot^{\cdot^{\cdot}} & \vdots \\ \frac{1}{b_0} & 0 & \cdots & 0 \end{bmatrix}. \quad (6)$$

Theorem 2 (Desired continuous-time state)**.** *Let* $B^{-1}(s)$ *in* (4) *be decomposed as*

$$B^{-1}(s) = F_s(s) + F_u(s), \quad (7)$$

with all poles $p_s \in \mathbb{C}$ *of* $F_s(s)$ *such that* $\Re(p_s) < 0$ *and all poles* $p_u \in \mathbb{C}$ *of* $F_u(s)$ *such that* $\Re(p_u) > 0$*. Let*

$$f_s(t) = \mathcal{L}^{-1}(F_s(s)), \quad f_u(t) = \mathcal{L}^{-1}(F_u(-s)), \quad (8a)$$

$$\hat{x}_{ccf,s}(t) = \int_{-\infty}^{t} f_s(t-\tau)\bar{r}(\tau)\,d\tau, \quad (8b)$$

$$\hat{x}_{ccf,u}(t) = \int_{t}^{\infty} f_u(t-\tau)\bar{r}(\tau)\,d\tau, \quad (8c)$$

where $\mathcal{L}^{-1}(\cdot)$ *is the inverse uni-lateral Laplace transform [15, Section 9.3]. Let* H_c *in* (4) *have realization* (5)*, then* $y(t) = C_c\hat{x}(t)$ *where*

$$\hat{x}(t) = T_{ccf}^{-1}(\hat{x}_{ccf,s}(t) + \hat{x}_{ccf,u}(t)), \quad (9)$$

is bounded and such that $\bar{y}(t) = \bar{r}(t)$*, with* $\bar{y}(t), \bar{r}(t)$ *in* (3)*.*

Proof. See [9, Section IV.B]. □

Theorem 2 provides the desired bounded state for optimal state tracking. Together with the state-space decomposition presented in the next section, Theorem 2 forms the basis of the proposed approach presented in Section VI.

Remark 1. *If poles of* $B^{-1}(s)$ *have* $\Re(p) = 0$*, i.e.,* $B^{-1}(s)$ *is non-hyperbolic, similar techniques as in [16] can be used.*

V. State-space decomposition

In this section, the multiplicative state-space decomposition is presented. Together with Theorem 2, the decomposition forms the basis of the proposed approach in Section VI.

Given the state-space system H in (2), the interest is in minimal realizations H_1, H_2 such that $H = H_1H_2$ in terms of state-space realization, where the zeros and poles of H can be arbitrarily assigned to H_1 or H_2. The starting point is the multiplicative decomposition $H = H_1H_2$ in terms of transfer functions as given by Lemma 3.

Lemma 3 (Transfer function decomposition)**.** *Let* $H \overset{z}{=} (A, B, C, D)$ *be a state-space realization with* n *states and invertible* D*. Let* $V \in \mathbb{R}^{n \times n_1}$ *be a column space of an invariant subspace of* A *and let* $V_\times \in \mathbb{R}^{n \times n_2}$ *be a column space of an invariant subspace of* $A_\times = A - BD^{-1}C$*, such that* $S = \begin{bmatrix} V & V_\times \end{bmatrix}$ *has full rank* $n = n_1 + n_2$*. Let*

$$\Pi = S \begin{bmatrix} I_{n_1} & 0_{n_1 \times n_2} \\ 0_{n_2 \times n_1} & 0_{n_2 \times n_2} \end{bmatrix} S^{-1}. \quad (10)$$

Then, the realizations

$$H_{1f} \overset{z}{=} \left[\begin{array}{c|c} A & \Pi BD^{-1} \\ \hline C & I \end{array}\right], \; H_{2f} \overset{z}{=} \left[\begin{array}{c|c} A & B \\ \hline C(I-\Pi) & D \end{array}\right] \quad (11)$$

are such that $H = H_{1f}H_{2f}$ *in terms of transfer functions, i.e.,* $C(zI-A)^{-1}B+D = (C(zI-A)^{-1}\Pi BD^{-1}+I)(C(I-\Pi)(zI-A)^{-1}B+D)$*.*

Proof. Extension of [17, Corrollary 11] to $D \neq I$. □

If the D matrix in Theorem 4 is singular, a bilinear transformation ([4, Section 3.4]; [15, Section 10.8.3]) can possibly be employed to obtain an equivalent system with nonsingular D matrix. A multiplicative decomposition for the transformed system is obtained through Lemma 3. Applying the inverse transformation on the decomposed system yields the decomposition for the original system since $\mathcal{B}(H_1H_2) = \mathcal{B}(H_1)\mathcal{B}(H_2)$.

Importantly, Lemma 3 guarantees equivalence in terms of transfer functions, but not in terms of state-space realizations. Indeed, the decomposition of Lemma 3 yields nonminimal realizations of H_{1f}, H_{2f} as both have state dimension n. By exploiting the modal form and using a suitable state transformation, the desired state-space decomposition for the proposed approach is obtained as given by Theorem 4.

Theorem 4 (State-space decomposition)**.** *Let* $T_{mod} \in \mathbb{C}^{n \times n}$ *be such that* $H_{mod} = \mathcal{T}(H, T_{mod}) = (A, B, C, D)$ *is in modal form [18, Section 7.4] with nonsingular* D*. Let* $H_{1f}H_{2f} = H_{mod}$ *be the decomposition given by Lemma 3. Let* $T_{per} \in \mathbb{R}^{n \times n}$ *be such that*

$$\mathcal{T}(H_{1f}, T_{per}) \overset{z}{=} \left[\begin{array}{cc|c} A_1 & 0 & B_1 \\ 0 & A_2 & 0 \\ \hline C_1 & C_{1r} & I \end{array}\right], \quad (12)$$

$$\mathcal{T}(H_{2f}, T_{per}) \overset{z}{=} \left[\begin{array}{cc|c} A_1 & 0 & B_{2r} \\ 0 & A_2 & B_2 \\ \hline 0 & C_2 & D \end{array}\right], \quad (13)$$

with $A_1 \in \mathbb{R}^{n_1 \times n_1}$*,* $A_2 \in \mathbb{R}^{n_2 \times n_2}$*,* $n_1 + n_2 = n$*, and define*

$$H_1 \overset{z}{=} \left[\begin{array}{c|c} A_1 & B_1 \\ \hline C_1 & I \end{array}\right], \qquad H_2 \overset{z}{=} \left[\begin{array}{c|c} A_2 & B_2 \\ \hline C_2 & D \end{array}\right]. \quad (14)$$

Furthermore, let $X \in \mathbb{R}^{n_1 \times n_2}$ *satisfy*

$$A_1X - XA_2 = B_1C_2. \quad (15)$$

Then, the state-space realization of $\mathcal{T}(H_1H_2, T_{per}^{-1}T_{12})$ *with*

$$T_{12} = \begin{bmatrix} I_{n_1} & X \\ 0_{n_1 \times n_2} & I_{n_2} \end{bmatrix}, \quad (16)$$

is identical to that of H_{mod}.

Proof. The minimal realizations follow from the modal form and T_{per} in (12) and (13). Furthermore, $\mathcal{T}(H_1H_2, T_{per}^{-1}T_{12}) = \mathcal{T}(\mathcal{T}(H_1H_2, T_{12}), T_{per}^{-1}) = H_{mod}$. □

Theorem 4 yields a state-space decomposition $H = H_1H_2$ with identical state-space realizations. Note that such a decomposition always exists. Together with Theorem 2, Theorem 4 forms the basis for the proposed approach presented in the next section.

Remark 2. *Note that V in Lemma 3 is related to the poles of H, whereas $V_\times$ is related to the zeros of H. Hence, the selection of $V, V_\times$ enables to assign the poles and zeros to either H_1 or H_2.*

VI. Approach

In the previous sections, preliminary results on the desired state and the state-space decomposition are presented. Based on these results, the proposed approach is presented in this section and special cases are recovered.

A. Exploiting stable inversion and multirate inversion

The proposed approach consists of two steps. First, stable inversion is applied to H_2 in (14) to obtain u such that $y_2[k] = u_1[k]$, for all k, see also Fig. 2. The solution is given by Theorem 5 and provides exact output tracking every sample. See [5, Section 4.2] for a proof.

Theorem 5 (Inversion of H_2)**.** *Consider Fig. 2 and let H_2^{-1} be given by*

$$\begin{bmatrix} x_s[k+1] \\ x_u[k+1] \end{bmatrix} = \begin{bmatrix} A_s & 0 \\ 0 & A_u \end{bmatrix} \begin{bmatrix} x_s[k] \\ x_u[k] \end{bmatrix} + \begin{bmatrix} B_s \\ B_u \end{bmatrix} u_1[k], \quad \text{(17a)}$$

$$u[k] = \begin{bmatrix} C_s & C_u \end{bmatrix} \begin{bmatrix} x_s[k] \\ x_u[k] \end{bmatrix} + Du_1[k], \quad \text{(17b)}$$

with $|\lambda(A_s)| < 1$ and $|\lambda(A_u)| > 1$. Then, $y_2[k] = u_1[k]$, for all k, if

$$u[k] = C_s x_s[k] + C_u x_u[k] + Du_1[k], \quad \text{(18)}$$

which is bounded for bounded u_1, where x_s follows from solving

$$x_s[k+1] = A_s x_s[k] + B_s u_1[k], \quad x_s[-\infty] = 0 \quad \text{(19)}$$

forward in time and x_u follows from solving

$$x_u[k+1] = A_u x_u[k] + B_u u_1[k], \quad x_u[\infty] = 0 \quad \text{(20)}$$

backward in time.

If u_1 is bounded, u in Theorem 5 is bounded by construction of x_s, x_u, even if H_2 is nonminimum phase. The stable inversion solution in Theorem 5 achieves exact output tracking every sample and has infinite preactuation. Regular causal inversion is recovered as special case if the system is minimum phase, i.e., x_u is non-existing, see also [5].

Second, multirate inversion is applied to H_1 in (14) to obtain u_1. Note that by Theorem 5, $y_2[k] = u_1[k]$, for all k. The solution is based on lifting the state equation over n_1 samples. The solution is given by Theorem 6 and provides exact state tracking every n_1 samples.

Theorem 6 (Inversion of H_1)**.** *Consider Fig. 2 with $y_2[k] = u_1[k]$, for all k, and let $\hat{x}_1$ be the desired state for system H_1 in* (14)*. Consider the state equation lifted over τ samples given by*

$$\underline{x}_1[q+1] = \underline{A}_1\, \underline{x}_1[q] + \underline{B}_1\, \underline{u}_1[q], \quad \text{(21)}$$

with $\underline{A}_1 = A_1^{n_1}$, $\underline{B}_1 = \begin{bmatrix} A_1^{n_1-1}B_1 & A_1^{n_1-2}B_1 & \dots & B_1 \end{bmatrix}$, $\underline{u}_1[q] = \begin{bmatrix} u_1[kn_1] & u_1[kn_1+1] & \dots & u_1[(k+1)n_1 - 1] \end{bmatrix}^\top$, and $\underline{x}_1[q] = x_1[kn_1]$. Then, $\underline{x}_1[q] = \hat{\underline{x}}_1[q]$, for all q, if

$$\underline{u}_1[q] = \underline{B}_1^{-1} \left(\hat{\underline{x}}_1[q+1] - \underline{A}_1\, \hat{\underline{x}}_1[q] \right), \quad \text{(22)}$$

which is bounded for bounded $\hat{x}_1$.

Proof. See [9, Section IV.C]. □

Importantly, the inversion approach in Theorem 6 is based on the continuous-time system H_c, rather than the discrete-time system H. The approach yields exact state tracking, and hence exact output tracking, every n_1 samples and has n_1 samples preactuation. Note that u_1 is bounded if $\hat{x}_1$ is bounded, even if H_1 is nonminimum phase. More details can be found in, for example, [9], [10]. The desired state $\hat{x}_1$ in Theorem 6 is obtained by Procedure 7 which follows from Section IV and Section V.

Procedure 7 (Desired state of H_1)**.** *Given H_c in* (5)*, H in* (2)*, and the decomposition $H = H_1H_2$ in Theorem 4, the following steps yields the desired state $\hat{x}_1[k]$ in Theorem 6.*

1) *Obtain the controllable canonical form $H_{ccf} = \mathcal{T}(H_c, T_{ccf})$ according to Lemma 1.*
2) *Obtain the desired state $\hat{x}(t)$ of H_c using Theorem 2.*
3) *Set the desired state of H to $\hat{x}[k] = \hat{x}(k\delta)$.*
4) *Obtain the desired state of H_{mod}: $\hat{x}_{mod}[k] = T_{mod}\hat{x}[k]$, with H_{mod}, T_{mod} in Theorem 4.*
5) *Given H_1, H_2 in* (14)*, let*

$$H_{12} = H_1H_2 \stackrel{z}{=} \left[\begin{array}{cc|c} A_1 & B_1C_2 & B_1D_2 \\ 0 & A_2 & B_2 \\ \hline C_1 & D_1C_2 & D_1D_2 \end{array} \right]. \quad \text{(23)}$$

6) *Obtain the desired state of H_{12}: $\hat{x}_{12}[k] = T_{12}^{-1}T_{per}\hat{x}_{mod}[k]$, with T_{12} in* (16) *and T_{per} satisfying* (12) *and* (13)*.*
7) *Obtain the desired state for H_1: $\hat{x}_1[k] = \begin{bmatrix} I_{n_1} & 0_{n_1\times n_2} \end{bmatrix} \hat{x}_{12}[k]$.*

The combination of the inversion of H_2 in Theorem 5 and the inversion of H_1 in Theorem 6 constitutes the control input u in Fig. 2, which is bounded by design, also for nonminimum-phase systems. The design freedom is in the decomposition of H into H_1 and H_2 in Theorem 4. Equation (23) shows that the output is given by $y[k] = C_1x_1[k] + D_1C_2x_2[k]$ since either $D_1 = 0$ or $D_2 = 0$ as $D = 0$ in (2). If $D_1 = 0$, $y[k] = C_1x_1[k]$ and since inversion of H_1 in Theorem 5 ensures tracking of x_1 every n_1 samples, there is perfect output tracking every n_1 samples. If $D_1 \neq 0$, $y[k]$ also depends on $x_2[k]$ of H_2 and since inversion of H_2 in

Theorem 6 does not provide perfect state tracking, there is no perfect output tracking for y every n_1 samples. Hence, to guarantee exact on-sample tracking every n_1 samples, $V, V_\times$ in Theorem 4 are preferably chosen such that $D_1 = 0$.

In summary, input $u[k]$ in Fig. 1 that minimizes $e(t)$, in terms of both the intersample and on-sample behavior, is obtained by decomposing H as in Fig. 2 using Theorem 4, followed by inversion of H_2 using Theorem 5 and inversion of H_1 using Theorem 6. In the next section, special cases are recovered.

Remark 3. *For strictly proper systems H_2, Theorem 5 can be applied to the bi-proper system $\bar{H}_2$ obtained through time shifts $\bar{H}_2 = z^{d_2} H_2$, where d_2 is the relative degree of H_2, see also [5, Remark 1]. If there are eigenvalues on the unit circle, i.e., there exist λ_i such that $|\lambda_i(A)| = 1$, then similar techniques as in [16] can be followed.*

Remark 4. *Note that $\underline{B}_1$ in Theorem 6 is the controllability matrix of H_1 and hence $\underline{B}_1^{-1}$ exists if H_1 is controllable.*

B. Special cases

The proposed approach provides a whole range of solutions as illustrated in Fig. 3. The stable inversion and multirate inversion solution are recovered as the two extreme cases and given by Corollary 8 and Corollary 9.

Corollary 8 (Special case: stable inversion [5])**.** *The stable inversion solution for H is recovered from the proposed approach in Section VI-A as special case when $H = H_2$, i.e., $H_1 = I$ and $n_1 = 0$.*

Corollary 9 (Special case: multirate inversion [9])**.** *The multirate inversion solution for H is recovered from the proposed approach in Section VI-A as special case when $H = H_1$, i.e., $H_2 = I$ and $n_1 = n$.*

Importantly, although Theorem 5 yields exact output tracking of H_2 for every sample, the inversion of H_1 does not reduce to conventional multirate inversion of H_1 since the desired state $\hat{x}_1$ depends on the full system H_c and not only on H_1.

The proposed approach provides a whole range of solutions that were non-existing before, see also Fig. 3. In the next section, the advantages are demonstrated by application to a motion system.

VII. Application to a Motion System

In this section, the approach proposed in Section VI is applied to a motion system. The results demonstrate the potential of the proposed approach.

A. Setup

The motion system is illustrated in Fig. 4(a) and based on the benchmark system in [5]. The continuous-time transfer function from input u to output y is given by

$$H_c = \frac{0.3125}{s^2} \frac{s^2 + 15s + 1500}{s^2 + 37.5s + 3750} \tag{24}$$

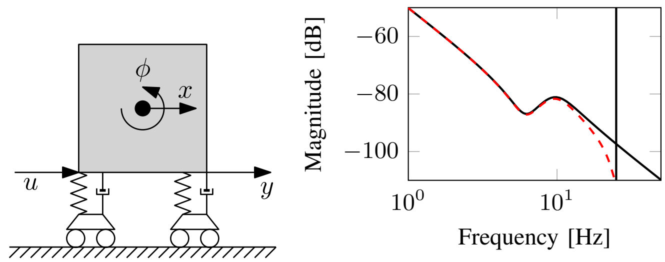

(a) The system is actuated by input force u, can translate in x direction, rotate in ϕ direction, and has output position y.

(b) Bode magnitude diagram of the continuous-time system H_c (——) and the discretized system H (- - -) from input u to output y in (a).

Fig. 4. Motion system used for validation of the proposed approach.

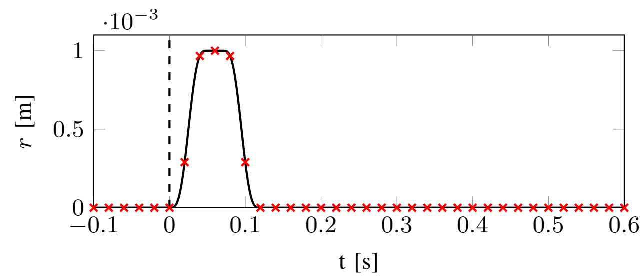

Fig. 5. The reference trajectory $r(t)$ (——), with discretization $r[k]$ (×). The trajectory consists of a forward and backward movement.

and is minimum phase. The discretized system (2) with sampling time $\delta = 0.02$ s has the transfer function

$$H = \frac{5.13 \times 10^{-5}(z + 0.842)}{(z-1)^2} \frac{z^2 - 1.249z + 0.742}{z^2 - 0.5415z + 0.4724} \tag{25}$$

and is also minimum phase. The Bode diagrams of H_c and H are shown in Fig. 4(b). Reference trajectory r is shown in Fig. 5. The system is controlled in open loop.

B. Results

Three different solutions are compared in simulation: the proposed approach with $n_1 = 2$, the special case $n_1 = 0$, i.e., stable inversion in Corollary 9, and the special case $n_1 = 4$, i.e., multirate inversion in Corollary 8. The error signals for the three approaches are shown in Fig. 6.

The results in Fig. 6(a) show that the special case of stable inversion achieves exact tracking every sample, but poor intersample behavior. The results for the special case of multirate inversion in Fig. 6(b) show good intersample behavior, but moderate on-sample behavior since the solution only yields exact tracking every $n = 4$ samples.

The results of the proposed approach are shown in Fig. 6(c). The results show good intersample behavior with exact on-sample tracking every $n_1 = 2$ samples. Hence, it outperforms the special case of multirate inversion in terms of on-sample performance. At the same time, it outperforms the special case of stable inversion in terms of intersample performance.

The results demonstrate the potential of the proposed approach on a motion system as it outperforms the existing solutions.

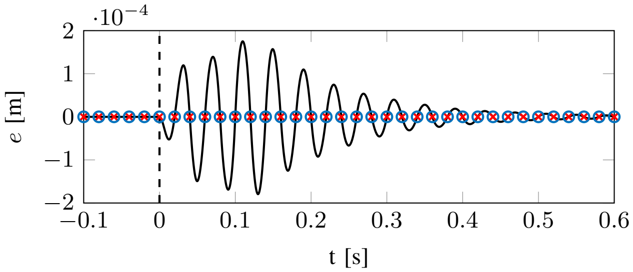

(a) Stable inversion yields exact on-sample tracking every sample (O), but poor intersample behavior (——).

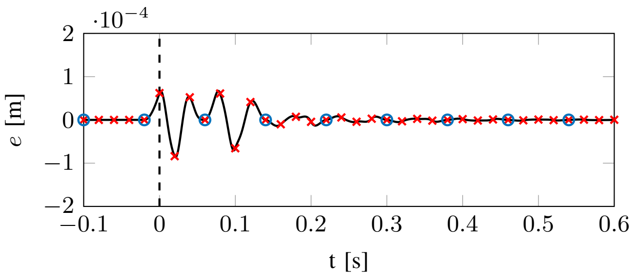

(b) Multirate inversion yields only exact on-sample tracking every $n = 4$ samples (O), but good intersample behavior (——).

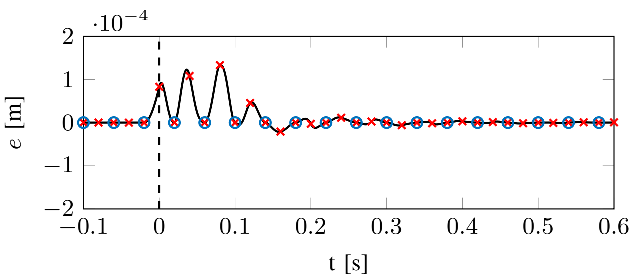

(c) The proposed approach yields exact on-sample tracking every $n_1 = 2$ samples (O) and good intersample behavior (——).

Fig. 6. Error signals with on-sample error $e[k]$ (×) and continuous-time error $e(t)$ (——).

VIII. Conclusion

A discrete-time system inversion approach is developed that balances the on-sample and intersample behavior for the purpose of continuous-time performance. The multirate inversion and stable inversion approaches are recovered as special cases. Application to a motion system demonstrates the advantages of the proposed approach.

In this paper, an multiplicative decomposition is considered. Ongoing research focuses on an additive decomposition of which preliminary results can be found in [19]. Ongoing research also focuses on extension to non-equidistantly sampled systems [20]. For these systems, which are essentially linear periodically time-varying (LPTV), poor intersample behavior is a well-known problem.

Acknowledgments

This work is part of the research programmes Robust Cyber-Physical Systems (RCPS) (No. 12694) and VIDI (No. 15698) which are both (partly) financed by the Netherlands Organisation for Scientific Research (NWO). The work is supported by JSPS KAKENHI Grant Number 18H05902.

References

[1] J. Butterworth, L. Pao, and D. Abramovitch, "Analysis and comparison of three discrete-time feedforward model-inverse control techniques for nonminimum-phase systems," *IFAC Mechatronics*, vol. 22, no. 5, pp. 577–587, 2012.

[2] G. M. Clayton, S. Tien, K. K. Leang, Q. Zou, and S. Devasia, "A Review of Feedforward Control Approaches in Nanopositioning for High-Speed SPM," *Journal of Dynamic Systems, Measurement, and Control*, vol. 131, no. 6, pp. 61 101:1–19, 2009.

[3] S. Devasia, D. Chen, and B. Paden, "Nonlinear Inversion-Based Output Tracking," *IEEE Transactions on Automatic Control*, vol. 41, no. 7, pp. 930–942, 1996.

[4] T. Chen and B. A. Francis, *Optimal Sampled-Data Control Systems*. London, Great Britain: Springer, 1995.

[5] J. van Zundert and T. Oomen, "On inversion-based approaches for feedforward and ILC," *IFAC Mechatronics*, vol. 50, pp. 282–291, 2018.

[6] K. L. Moore, S. Bhattacharyya, and M. Dahleh, "Capabilities and Limitations of Multirate Control Schemes," *Automatica*, vol. 29, no. 4, pp. 941–951, 1993.

[7] T. Oomen, J. van de Wijdeven, and O. Bosgra, "Suppressing intersample behavior in iterative learning control," *Automatica*, vol. 45, no. 4, pp. 981–988, 2009.

[8] J. A. Butterworth, L. Y. Pao, and D. Y. Abramovitch, "The Effect of Nonminimum-Phase Zero Locations on the Performance of Feedforward Model-Inverse Control Techniques in Discrete-Time Systems," in *Proceedings of the 2008 American Control Conference*, Seattle, Washington, 2008, pp. 2696–2702.

[9] W. Ohnishi, T. Beauduin, and H. Fujimoto, "Preactuated Multirate Feedforward Control for Independent Stable Inversion of Unstable Intrinsic and Discretization Zeros," *IEEE/ASME Transactions on Mechatronics*, 2019, DOI: 10.1109/TMECH.2019.2896237.

[10] H. Fujimoto, Y. Hori, and A. Kawamura, "Perfect Tracking Control Based on Multirate Feedforward Control with Generalized Sampling Periods," *IEEE Transactions on Industrial Electronics*, vol. 48, no. 3, pp. 636–644, 2001.

[11] J. van Zundert, T. Oomen, J. Verhaegh, W. Aangenent, D. J. Antunes, and W. Heemels, "Beyond Performance/Cost Tradeoffs in Motion Control: A Multirate Feedforward Design with Application to a Dual-Stage Wafer System," *IEEE Transactions on Control Systems Technology*, 2018, DOI: 10.1109/TCST.2018.2882341.

[12] Y. Yamamoto, "A Function Space Approach to Sampled Data Control Systems and Tracking Problems," *IEEE Transactions on Automatic Control*, vol. 39, no. 4, pp. 703–713, 1994.

[13] B. A. Bamieh and J. B. Pearson Jr., "A General Framework for Linear Periodic Systems with Applications to H^∞ Sampled-Data Control," *IEEE Transactions on Automatic Control*, vol. 37, no. 4, pp. 418–435, 1992.

[14] G. C. Goodwin, S. F. Graebe, and M. E. Salgado, *Control System Design*. Upper Saddle River, New Jersey, 2000.

[15] A. V. Oppenheim, A. S. Willsky, and S. H. Nawab, *Signals and Systems*, 2nd ed. Prentice-Hall, Inc., 1997.

[16] S. Devasia, "Output Tracking with Nonhyperbolic and Near Nonhyperbolic Internal Dynamics: Helicopter Hover Control," in *Proceedings of the 1997 American Control Conference*, Albuquerque, New Mexico, 1997, pp. 1439–1446.

[17] H. Bart, I. Gohberg, M. Kaashoek, and A. Ran, "Schur complements and state space realizations," *Linear Algebra and its Applications*, vol. 399, pp. 203–224, 2005.

[18] G. F. Franklin, J. D. Powell, and A. Emami-Naeini, *Feedback Control of Dynamic Systems*, 7th ed. Upper Saddle River, New Jersey: Pearson, 2015.

[19] W. Ohnishi and H. Fujimoto, "Multirate Feedforward Control Based on Modal Form," in *Conference on Control Technology and Applications*, Copenhagen, Denmark, 2018, pp. 1120–1125.

[20] J. van Zundert and T. Oomen, "LPTV Loop-Shaping with Application to Non-Equidistantly Sampled Precision Mechatronics," in *Proceedings of the 15th International Workshop on Advanced Motion Control*, Tokyo, Japan, 2018, pp. 467–472.